

# Alternative Mechanisms in Hydrogen Production by Aluminum Anion Clusters

Paul N. Day,<sup>\*,†,‡</sup> Kiet A. Nguyen,<sup>†,§</sup> and Ruth Pachter<sup>\*,†</sup>

<sup>†</sup>Materials and Manufacturing Directorate, Air Force Research Laboratory, Wright Patterson Air Force Base, Ohio 45433, United States

<sup>‡</sup>General Dynamics Information Technology, Inc., Dayton, Ohio 45431, United States

<sup>§</sup>UES, Inc., Dayton, Ohio 45432, United States

 Supporting Information

**ABSTRACT:** Possible mechanisms for the reaction of aluminum anion clusters with water have been studied theoretically using density functional theory for four different size clusters. Our results confirm the previously found (Reber et al. *J. Phys. Chem. A* **2010**, *114*, 6071) importance of Lewis-acid and Lewis-base sites on the cluster in the size specificity of the reactivity. However, alternative viable mechanisms have been found using both Langmuir–Hinshelwood and Eley–Rideal kinetics. Grotthuss-like mechanisms appear to be the most energetically favorable. We show that while the superatom theory successfully predicts reactivity of smaller clusters, it is less useful for the larger clusters.

## I. INTRODUCTION

The reaction of aluminum with water to produce hydrogen gas is of interest as an alternative energy source. While aluminum in bulk reacts too slowly for practical applications, evidence suggests much faster rates for micro- or nano-sized aluminum particles.<sup>1,2</sup> As with other metal nanoparticles, structure and properties vary by cluster size, and these variations may be at least partially explained or predicted through the use of “super-atom” theory and “magic numbers”, which are related to the spherical jellium model.<sup>3–8</sup> In the superatom theory, the valence electrons in a cluster of metal atoms are sufficiently delocalized such that the wave function solution, in analogy with atomic wave functions, fills “super-atom” electronic shells designated as 1S, 1P, 1D, 2S, 1F, 2P, 1G, 2D, 3S, ..., thus generating the following series of magic numbers: 2, 8, 18, 20, 34, 40, 58, 68, 70, ... A cluster with a magic number of valence electrons should be particularly stable, in analogy with an inert gas. The aluminum atom has three valence electrons, and the superatom theory correctly predicts the inertness of  $\text{Al}_{13}^{-1}$ , with 40 valence electrons, as well as of  $\text{Al}_{11}^{-1}$ , with 34 valence electrons. The high reactivity of  $\text{Al}_{12}^{-1}$ , with 37 valence electrons, and of  $\text{Al}_{17}^{-1}$ , with 52 valence electrons, is also consistent with the theory.

The production of hydrogen gas from the reaction of aluminum nanoclusters with water was observed in a fast-flow reactor.<sup>9,10</sup> Reber et al.<sup>10</sup> investigated possible correlations between the reactivity with water and various calculated properties of the clusters, including dipole moment, binding energy, transition state energy, product energy, and orbital energies. The  $\text{Al}_{12}^{-1}$  cluster has a relatively large dipole moment and reacts rapidly with water (although apparently does not produce  $\text{H}_2$ ), but the symmetric  $\text{Al}_{17}^{-1}$  has a zero dipole moment and also reacts rapidly with water, including the release of  $\text{H}_2$ .

The  $\text{Al}_{12}^{-1}$  cluster also has a large binding energy with water and a low barrier for the OH bond-breaking, but these properties alone are not sufficient to predict the reactivity for each cluster size. The energy and structure of the Kohn–Sham molecular

orbitals were found to be important, particularly that of the highest occupied molecular orbital (HOMO) and lowest unoccupied molecular orbital (LUMO). In systems with an odd number of electrons ( $\text{Al}_{12}^{-1}$  and  $\text{Al}_{20}^{-1}$ ), the singularly occupied molecular orbital will be labeled SOMO, the lowest completely unoccupied orbital LUMO, and the highest doubly occupied orbital SOMO–1. Positions on the cluster where the LUMO protrudes out in space are Lewis-acid sites, which tend to attract the lone-pair of electrons of the oxygen atom in the water molecule. A water molecule will bind at these sites with a typical stabilization energy of 0.3–0.6 eV. If an adjacent aluminum atom has a strong contribution from the HOMO (the SOMO for odd-electron species), it can act as a Lewis-base, and one of the hydrogen atoms from the water molecule can bind to it, breaking its bond to the oxygen atom, resulting in the H and the OH being bound on adjacent aluminum atoms. For some clusters, the barrier for this reaction is less than the stabilization energy of the initial water binding, and this step is exothermic by over 1.0 eV, making the reaction thermally favorable. Other water molecules can react with other Lewis-acid–Lewis-base pairs on the aluminum cluster. Because of the exothermicity of this reaction, the system may have enough energy for two hydrogen atoms on adjacent aluminum atoms to form a bond and be released as  $\text{H}_2$ . This is the Langmuir–Hinshelwood (LH) mechanism described by Reber et al.<sup>10</sup> Alternative mechanisms that they describe include the Eley–Rideal (ER) type, where the second water molecule does not undergo bond-breaking on the surface but instead transfers a hydrogen atom directly to the bound hydrogen to form  $\text{H}_2$ , and a “direct” mechanism, where neither water molecule undergoes surface bond-breaking but instead each directly contributes a hydrogen atom to form  $\text{H}_2$ . In studies utilizing molecular dynamics (MD),<sup>11,12</sup> a lower barrier for the first step of the reaction was found through a Grotthuss-like

**Received:** September 27, 2011

**Published:** November 22, 2011

mechanism where one, two, or three extra water molecules assist in the transfer of the hydrogen atom. This mechanism may be combined with either the LH or the ER mechanism to form a complete path for the formation of H<sub>2</sub>.

In this study, we investigate the reaction of water with aluminum cluster anions of size  $n = 12, 17, 20$ , and  $23$ , by using density functional theory and searching for viable reaction paths to produce H<sub>2</sub>, taking all of the possible mechanistic paths into account. The reactions with  $n = 12$  and  $n = 17$  have been studied previously both experimentally and theoretically, and we expand upon those results. For  $n = 23$ , the number of valence electrons corresponds to the magic number of  $70$ , so the superatom theory predicts it should be inert, but experiment has reported it to be highly reactive with water.<sup>10</sup> Conversely, Al<sub>20</sub><sup>-1</sup>, with  $60$  valence electrons, should be reactive, but has been reported to have low reactivity.<sup>10</sup> Apparently, other structural or dynamic factors prevail over the superatom theory for these clusters. This is consistent with the results of Ma et al.,<sup>13</sup> where in a study of the photoelectron spectra of aluminum cluster anions in the size range  $n = 13\text{--}75$ , only a few select cluster sizes followed the superatom model.

## II. COMPUTATIONAL METHODS

For Al<sub>12</sub><sup>-1</sup> and Al<sub>17</sub><sup>-1</sup>, the structures of Roach et al.<sup>9</sup> were used as starting points for the optimized structures. The structures found by Aguado and Lopez<sup>14</sup> were used as starting points for the minimum energy structures of Al<sub>20</sub><sup>-1</sup> and Al<sub>23</sub><sup>-1</sup>, as well as confirmation of the Al<sub>17</sub><sup>-1</sup> structure. The PBE<sup>15,16</sup> functional was used in the previous studies, and thus we report results with this functional to extend the previous results. In a study by Drebov and Ahlrichs,<sup>17</sup> high-level ab initio calculations were carried out on small neutral aluminum clusters, and the results were used to test several exchange-correlation functionals. Because they did not include any meta-hybrid functionals in this study, we have extended their results by testing the M06 and M06-2X functionals of Zhao and Truhlar.<sup>18</sup> The results are listed in Table S1 of the Supporting Information, including the cohesive energies and the dissociation energies as well as the maximum error and average error for each. The M06 functional, which has  $27\%$  exact exchange and has been parametrized to be accurate for both metallic and organic systems, has lower errors in each category than does the M06-2X functional, which has  $54\%$  exact exchange and has been parametrized primarily for main group chemistry. The M06 functional has the lowest maximum error and lowest average error of any functional for the cohesive energy, and it has the second lowest maximum error and the lowest average error for the dissociation energy; thus it was chosen for this study. Reaction paths are reported for the Al<sub>12</sub><sup>-1</sup> and Al<sub>17</sub><sup>-1</sup> systems using the PBE<sup>15,16</sup> and M06<sup>18</sup> functionals with the 6-311++G\*\* basis set. For the Al<sub>20</sub><sup>-1</sup> and Al<sub>23</sub><sup>-1</sup> systems, results are calculated at the PBE/6-311G\*\* and M06/6-311++G\*\* levels of theory. All calculations were carried out with the GAMESS<sup>19</sup> program except for the M06 calculations on Al<sub>17</sub><sup>-1</sup>, Al<sub>20</sub><sup>-1</sup>, and Al<sub>23</sub><sup>-1</sup>, which were carried out with Gaussian 09.<sup>20</sup>

The potential energy surface for each Al <sub>$n$</sub> <sup>-1</sup>-H<sub>2</sub>O system was sampled by carrying out DFT local optimizations with the water molecule near each aluminum atom. Only sites with significant LUMO or LUMO+1 contribution had a binding interaction. For the Grothuss-type mechanisms, only one additional water molecule was included for each step. While mechanisms with additional water molecules probably exist, a previous study<sup>11</sup>

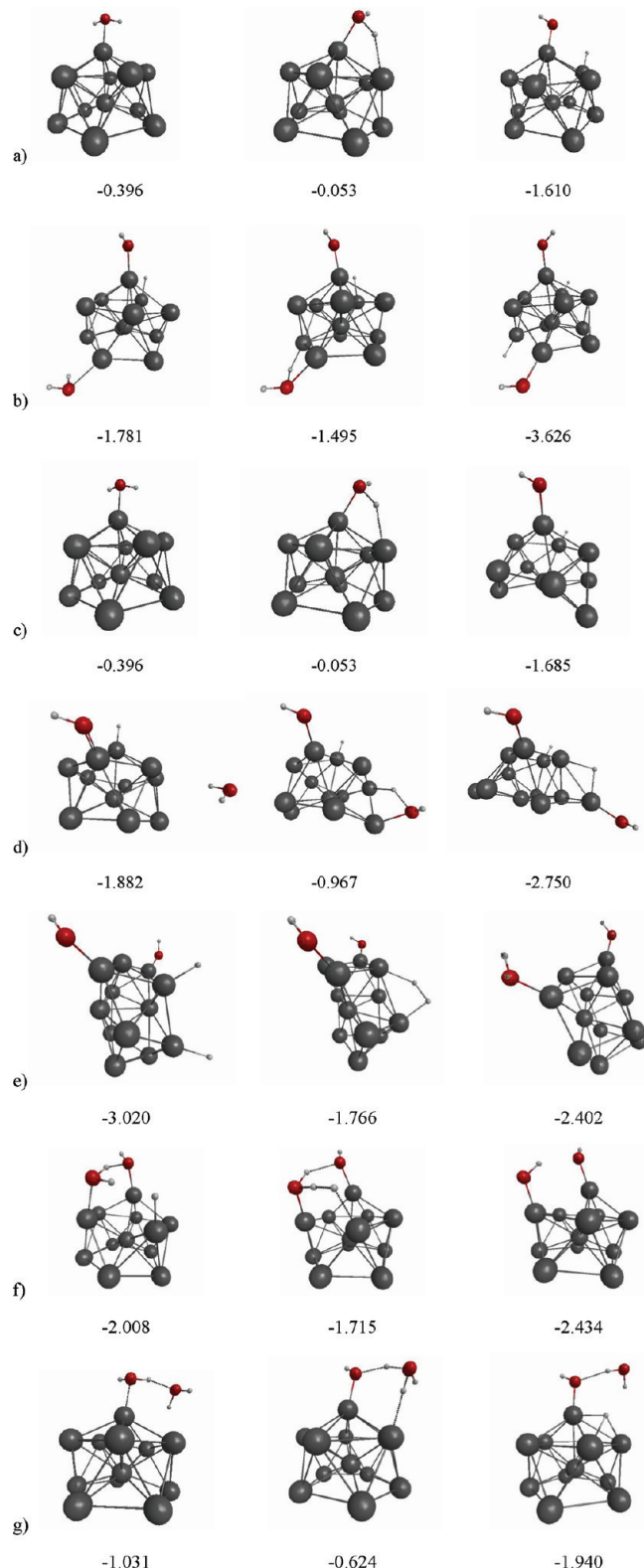


**Figure 1.** Reaction path structures for Al<sub>12</sub><sup>-1</sup> + water. Each row of this figure has the reactant, transition state, and product structures for the given step. The relative enthalpy, calculated with M06, is listed under each structure (eV). (a) Step 1 for LH1 and ER. (b) LH1 step 2. (c) LH2 step 1. (d) LH2 step 2. (e) LH2 step 3. (f) ER step 2. (g) GLH step 1.

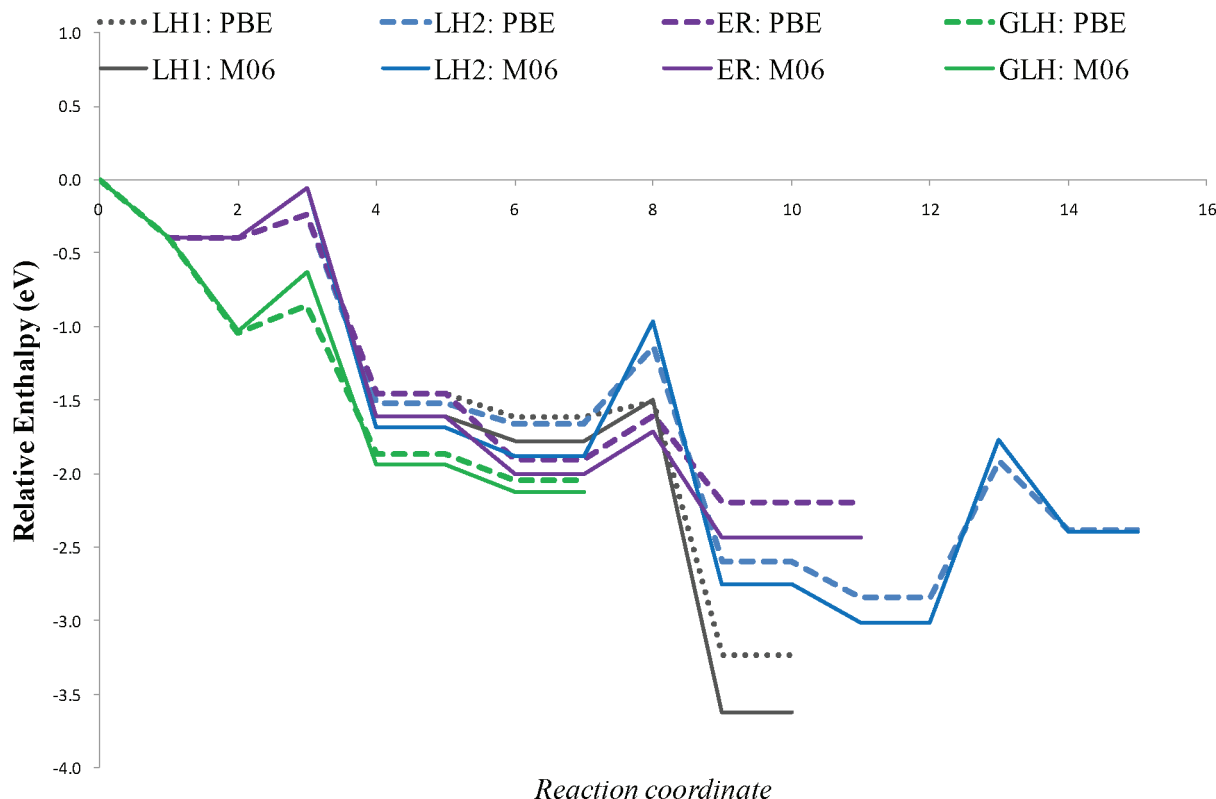


**Figure 2.** PBE and M06 reaction path energetics (corrected with zero-point-vibrational energies) with the 6-311++G\*\* basis set for  $\text{Al}_{12}^{-1}$  + water. The LH1 mechanism is consistent with Roach et al.<sup>9</sup> and does not release  $\text{H}_2$ , while the GLH mechanism ends when the second water molecule does not form an Al–O bond. The other two mechanisms release  $\text{H}_2$ .

found the lowest barrier with just one additional water molecule. The transition states for each mechanism were found by the standard search methods<sup>21–23</sup> available in the GAMESS and Gaussian programs, and each transition state was confirmed to have exactly one imaginary frequency. Reaction path following calculations<sup>24</sup> were carried out to confirm that the transition state connects the reactant to the product.

### III. RESULTS AND DISCUSSION

**A.  $\text{Al}_{12}^{-1}$ .** The extremely stable “super halide” ion  $\text{Al}_{13}^{-1}$  has an icosohedral structure with one atom in the center and the other 12 atoms located at the icosohedron’s vertices, and the  $\text{Al}_{12}^{-1}$  ion has a similar structure with one of the vertex atoms missing; thus it can be described as two stacked, staggered pentagonal rings with one atom on top and one central atom.

The LUMO for the  $\text{Al}_{12}^{-1}$  cluster has a large, protruding lobe on the “top” atom, and thus the oxygen atom of the water molecules binds to this aluminum atom, as found previously,<sup>9,10</sup> and an O–H bond is broken when one hydrogen atom binds to an adjacent aluminum atom. Reactant, transition state, and product structures for each step in each reaction mechanism studied here are shown in Figure 1, as well as the enthalpy relative to the original reactants. Figure 2 shows the energetics along each reaction path. Two different structures with similar energies were found for the product of the first step. When the geometry optimization was carried out with the pure GGA functional PBE, the structure shown as the product of step1:LH1 was found, which appears to correspond to the structure found previously.<sup>9,10</sup> When the optimization was carried out with a hybrid functional,

the system rearranged to the structure shown as the product of step1:LH2, where the bottom ring of aluminum atoms, instead of resembling a pentagon, now resembles a hexagon with one atom missing. When the two structures were reoptimized at each level of theory, they were found to have similar energies, with the LH2 structure lower in energy by 0.08 eV with either the PBE or the M06 functional. When the LH1 structure is used, the reaction proceeds as found previously,<sup>9,10</sup> with the second water molecule binding to a site opposite the first water molecule, and the second attached hydrogen atom being too distant from the first hydrogen atom for a viable reaction path to release  $\text{H}_2$ . However, when the LH2 structure is used, the second water molecule binds such that when the O–H bond splits, this second attached hydrogen atom is adjacent to the first one. The barrier for this second bond-breaking step is higher in LH2 than in LH1, but with the two hydrogen atoms in closer proximity in the LH2 mechanism, a path could be found where  $\text{H}_2$  is released.

A reaction path was also found that follows the ER type mechanism in the second step. This mechanism follows the same mechanism as LH1 for the first step. As can be seen in Figure 1, in the second step of the ER mechanism, the second water molecule directly transfers a hydrogen atom to the aluminum-bound hydrogen atom from the first step, thus creating  $\text{H}_2$  in just two steps. Because of hydrogen bonding with the other oxygen atom, the addition of the second water molecule to the cluster in the ER mechanism has an additional stabilization energy, 0.4 eV as compared to 0.2 eV for LH1 or LH2. The ER mechanism also has a low barrier for the second step, 0.3 eV, as compared to 0.5 eV for LH2 (M06: 0.9 eV). The barrier for the second step in LH1 is 0.1 eV (M06: 0.3 eV), but this mechanism does not lead to the release of  $\text{H}_2$ .

The molecular dynamics study of Shimajo et al.<sup>11</sup> showed that, for the first OH bond-breaking step, the Grotthuss-like mechanism with one, two, or three additional water molecules has a lower barrier than the LH mechanism (zero additional water molecules), with the lowest barrier being with one additional water molecule, followed by two additional water molecules, and then three. We found that while one additional water molecule

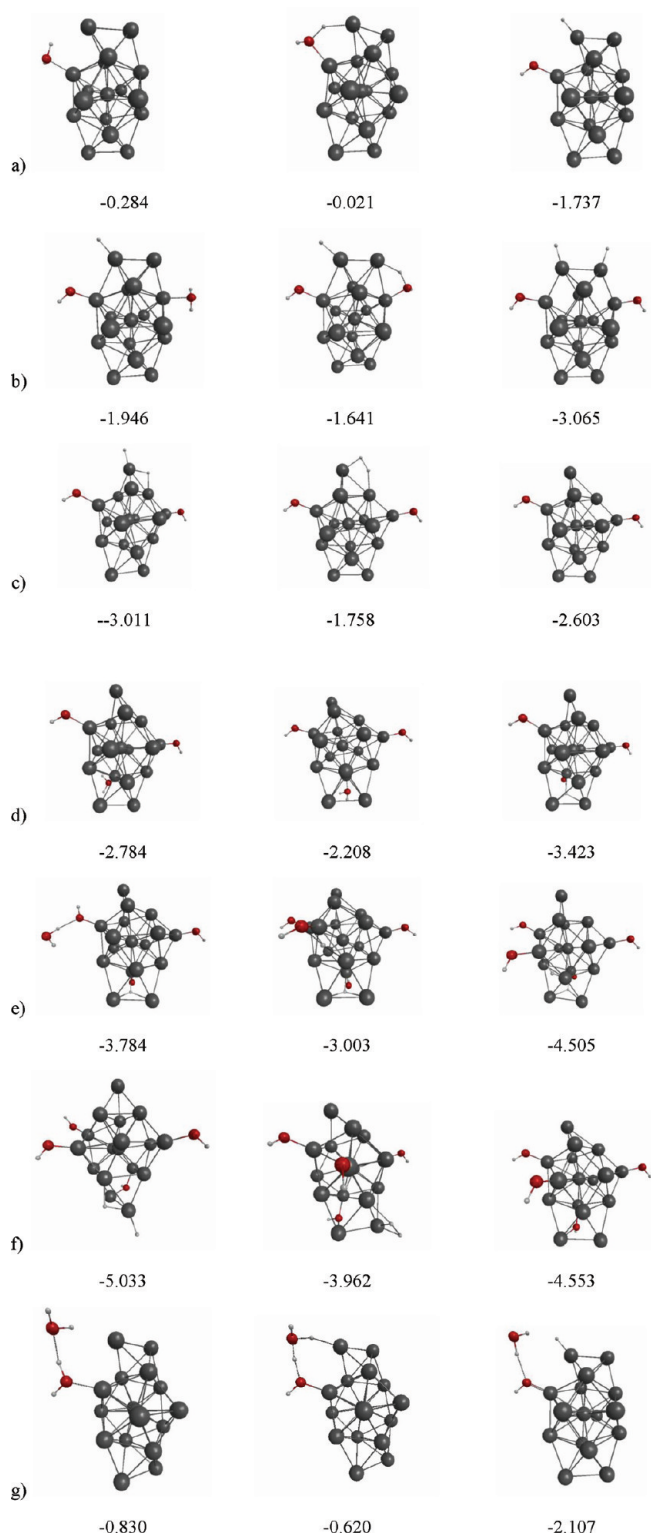
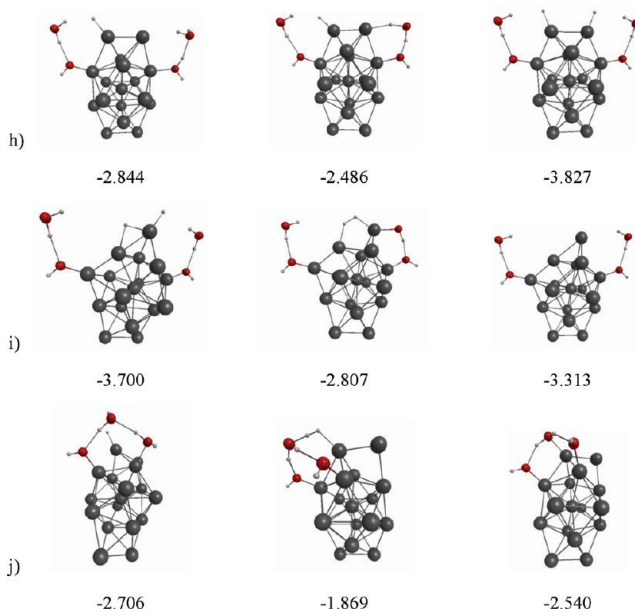


Figure 3. Continued



**Figure 3.** Reaction path structures for  $\text{Al}_{17}^{-1}$  + water. See caption for Figure 1. (a) LH step 1. (b) LH step 2. (c) LH step 3. (d) LH step 4. (e) LH step 5. (f) LH step 6. (g) GLH and GER step 1. (h) GLH step 2. (i) GLH step 3. (j) GER step 2.

provides stabilization energy of about 0.6 eV due to hydrogen bonding, the barrier for the first step is similar in both mechanisms, close to 0.2 eV (M06: 0.4 eV). However, a mechanism that completes the reaction using the Grotthuss-like mechanism could not be found for the  $\text{Al}_{12}^{-1}$  cluster. Only the first step in a possible GLH or GER mechanism was found. Thus, the ER mechanism seems most likely in this case.

Results from the PBE functional and the M06 functional are generally in good agreement. One difference is that the reaction barriers are slightly larger when the M06 functional is used. This could be expected because GGA functionals usually underestimate transition state energies. Also, for the final configuration of the LH1 mechanism, the M06 functional yields a lower energy. The particularly low energy for the final product of this mechanism, which does not release  $\text{H}_2$ , may be the explanation for the experimental evidence that this cluster does not produce  $\text{H}_2$ .

**B.  $\text{Al}_{17}^{-1}$ .** The minimum energy structure for  $\text{Al}_{17}^{-1}$  identified by Aguado and Lopez<sup>14</sup> consists of an icosahedral  $\text{Al}_{13}^{-1}$  core with a two-atom capping bridge and an identical capping bridge opposite the first one, creating a prolate structure with nearly  $D_{2h}$  symmetry. The capping atoms are Lewis-base sites, while the adjacent “side” atoms (those coordinated to just one of the capping atoms) are the Lewis-acid sites.

Three mechanisms have been found for the release of  $\text{H}_2$ : LH, GLH, and GER. Figure 3 gives the structure and relative enthalpy for the reactant, transition state, and product of each step in each mechanism, and the energetics are plotted in Figure 4. The two functionals are in good agreement, with the main difference being the larger barriers in the M06 calculations. An unassisted ER mechanism is not feasible due to the distance between the second Lewis-acid site and the first Lewis-base site. The LH mechanism was identified previously,<sup>9,10</sup> but here we have extended it to the release of a second  $\text{H}_2$  molecule. The two Grotthuss-like mechanisms each have one additional water

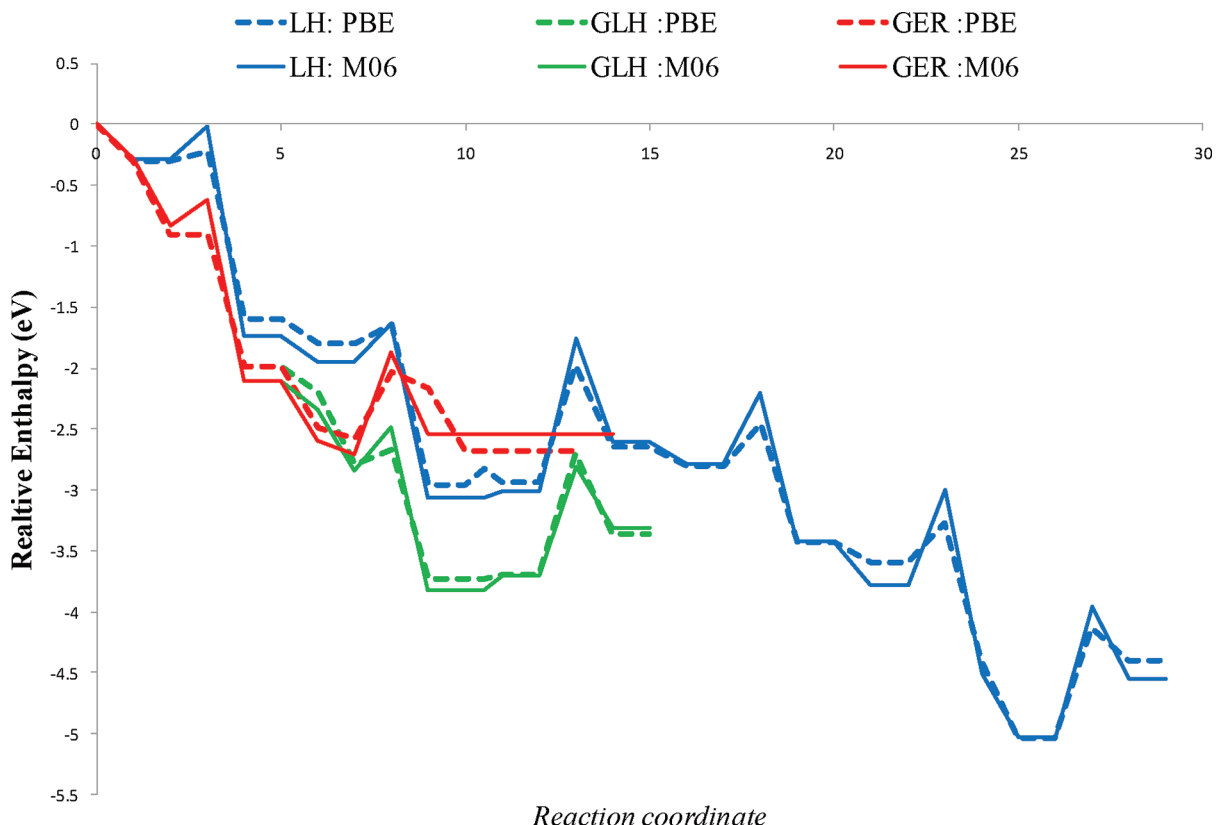


**Figure 4.** PBE and M06 reaction path energetics with the 6-311++G<sup>\*\*</sup> basis set for  $\text{Al}_{17}^{-1}$  + water. The first three steps of the LH mechanism, which results in production of a  $\text{H}_2$  molecule, are consistent with the previous results,<sup>9,10</sup> but here the mechanism has been extended to the release of a second  $\text{H}_2$  molecule. The GLH and GER mechanisms shown each release a  $\text{H}_2$  molecule.

molecule assisting in the first O–H bond-breaking step, and appear energetically favorable, as the hydrogen bonding of the additional water provides an additional 0.6 eV in stabilization energy and the first barrier is reduced from 0.08 eV (M06: 0.26 eV) to 0.00 eV (M06: 0.21 eV). While the reaction path for the release of the  $\text{H}_2$  molecule by the LH mechanism involves adsorption of a second water molecule with an exothermicity of 0.2 eV, in the GLH mechanism the third and fourth water molecules are adsorbed with an exothermicity of 0.8 eV, and in the GER mechanism the third water molecule is adsorbed with an exothermicity of 0.6 eV. The LH and GLH mechanisms each have a second step with a small barrier around 0.1 eV (M06: 0.3 eV) and an exothermicity around 1 eV, followed by a third step with a barrier of about 1.0 eV and an endothermicity of 0.3 eV (M06: 0.4 eV). The GER mechanism has only two steps, with the second and final step having a barrier of 0.54 eV (M06: 0.84 eV) and a small exothermicity of about 0.1 eV. While the GER mechanism might be preferred as part of a renewable energy cycle, where the lower overall change in energy results in a faster reaction rate,<sup>25</sup> the GLH mechanism's lower barrier for the second step, as well as the larger overall exothermicity, makes it appear energetically favorable. Also, the experimental results<sup>9,10</sup> indicate that the GLH mechanism is preferred over the GER mechanism, as the peak at a mass of 535 is more prominent than a peak at 515. The GLH mechanism might be preferred if the additional heat of reaction can be utilized and if the aluminum hydroxide product is desired. A recent MD simulation by Ohmura et al.<sup>12</sup> shows this system producing three  $\text{H}_2$  molecules.

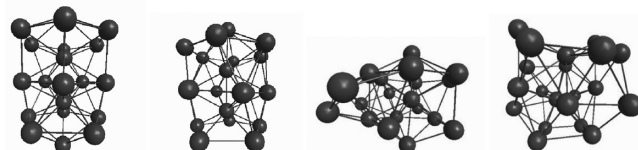


**Figure 5.** Structures for  $\text{Al}_{20}^{-1}$ , from left to right: M1, M2, M3, and M4.

Their mechanism for producing the first  $\text{H}_2$  molecule appears to be an alternative GER mechanism, where the first Al–H bond is formed in a Grotthuss-like step similar to that shown here, while the second step has a water molecule bind to an adjacent Al atom and transfer one of its H atoms to this bound H atom in a manner similar to the ER mechanism, but with some influence from other water molecules. Because their figures<sup>12</sup> do not show the full cluster or all of the water molecules involved, a full comparison with our results is not possible.

The LH mechanism has been extended for the release of a second  $\text{H}_2$  molecule. The reaction path to release the second  $\text{H}_2$  has higher barriers and less exothermicity than the path for the first  $\text{H}_2$ . However, it should still be feasible because releasing the first  $\text{H}_2$  was exothermic by 2.6 eV, and release of the second  $\text{H}_2$  is exothermic by about 2 eV.

**C.  $\text{Al}_{20}^{-1}$ .** The four energy-minimized structures for  $n = 20$  reported by Aguado and Lopez<sup>14</sup> are shown in Figure 5. The first minima, labeled M1 in Figure 5, was found to be lowest in energy for the neutral, the cation, and the anion, and our calculations

**Table 1.** Relative Energies of  $\text{Al}_{20}^{-1}$  Structures

		M1	M2	M3	M4
M06/6-311++G**	energy (eV)	0.00	1.08	0.86	1.15
	enthalpy (eV)	0.00	1.04	0.85	1.12
PBE/6-311G**	energy (eV)	0.00	0.73	0.82	0.88
	enthalpy (eV)	0.00	0.73	0.83	0.87
PBE/DZP	ref 14	0.00	0.89	0.87	0.91

with both the PBE and the M06 functionals also found this structure to be lowest in energy for the anion, as shown in Table 1. This structure can be approximately described as the icosohedral structure of  $\text{Al}_{13}^{-1}$  with a hexagonal ring stacked on top and a single atom stacked on top of that. Thus, it has the stacking sequence 1–5–1–5–1–6–1. The structure M2 has the stacking sequence 5–1–6–1–6–1 and has an energy about 1 eV higher than that of structure M1. Structure M3 could be described as being composed of a 1–5–1–6–1 stack, with the remaining 6 atoms forming a floppy wing on one side. M3 was found to be second lowest in energy when the M06 functional was used, but still 0.8 eV less stable than M1. Structure M4 might be roughly described by the stacking sequence 4–1–7–1–7, and it has an energy 1.1 eV above the energy of M1. Four types of mechanisms have been found for the reaction of structure M1 with water to produce  $\text{H}_2$ : LH, ER, GLH, and GER. The structures for these mechanisms are shown in Figure 6 along with the relative enthalpies, and the energetics are plotted in Figure 7. The atom in the hexagonal ring that is most evenly staggered between two atoms in the pentagonal ring below is the most electron deficient, and thus it has a protruding lobe in the LUMO. This is where the oxygen atom of a water molecule is most likely to interact. The SOMO has a large lobe on the top atom, and the OH bond can cleave across this pair of adjacent Lewis-acid–Lewis-base sites. This step is identical in the LH and ER mechanisms, while in the GLH and GER mechanisms, an additional water molecule facilitates the transfer of the hydrogen atom, significantly lowering the barrier.

In the first step for the LH and ER mechanisms, the barrier is 0.47 eV (M06: 0.80 eV), which is greater than the 0.3 eV (M06: 0.14 eV) gained by the initial coordination of the water molecule, implying a low reaction rate for these mechanisms except at high temperature. However, this step is exothermic by 1.3 eV, which should make the rest of either reaction path feasible. In the LH mechanism, coordination of second water molecule gains another 0.44 eV (M06: 0.26 eV), while the second O–H bond-breaking barrier is 0.48 eV (M06: 0.55 eV). This step is exothermic by 0.43 eV (M06: 0.97 eV). The third step, where the  $\text{H}_2$  leaves, has a barrier of 1.33 eV (M06: 1.77 eV), in a step that is endothermic by 0.44 eV (M06: 0.92 eV). This mechanism has an overall exothermicity of 2.44 eV (M06: 1.89 eV). In the ER mechanism, the second water attaches to an aluminum atom adjacent to the already attached OH and H, and a hydrogen bond is formed by the nonreacting hydrogen atom to the first oxygen atom, resulting in a complex slightly more stable than in the LH mechanism. The second step has a larger barrier than the second step in the LH mechanism, but is also the final step, releasing  $\text{H}_2$ . A slight variant of the ER mechanism was also found, where the second water molecule does not form the additional hydrogen bond, making this intermediate state slightly less stable, resulting in a smaller exothermicity for its formation but then a slightly smaller barrier for the final step. The ER mechanisms seem more

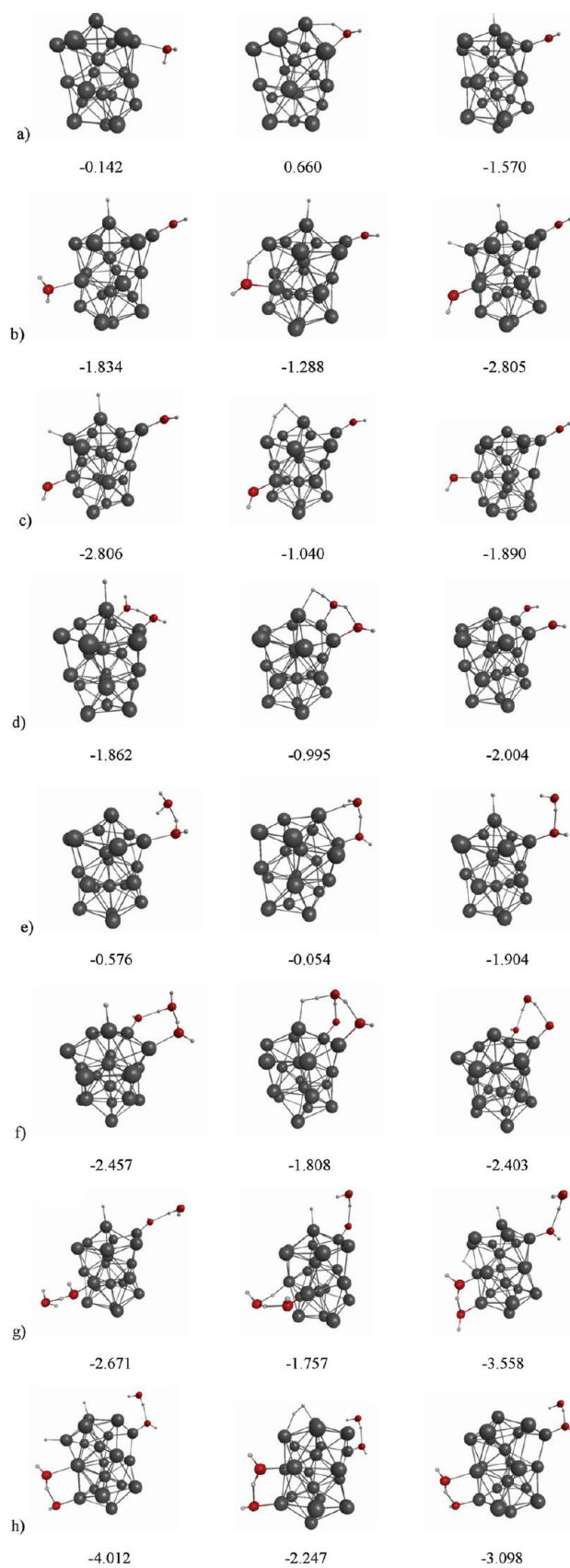


**Figure 6.** Reaction path structures for  $\text{Al}_{20}^{-1} + \text{water}$ . See caption for Figure 1. (a) LH and ER step 1. (b) LH step 2. (c) LH step 3. (d) ER step 2. (e) GLH and GER step 1. (f) GER step 2. (g) GLH step 2. (h) GLH step 3.

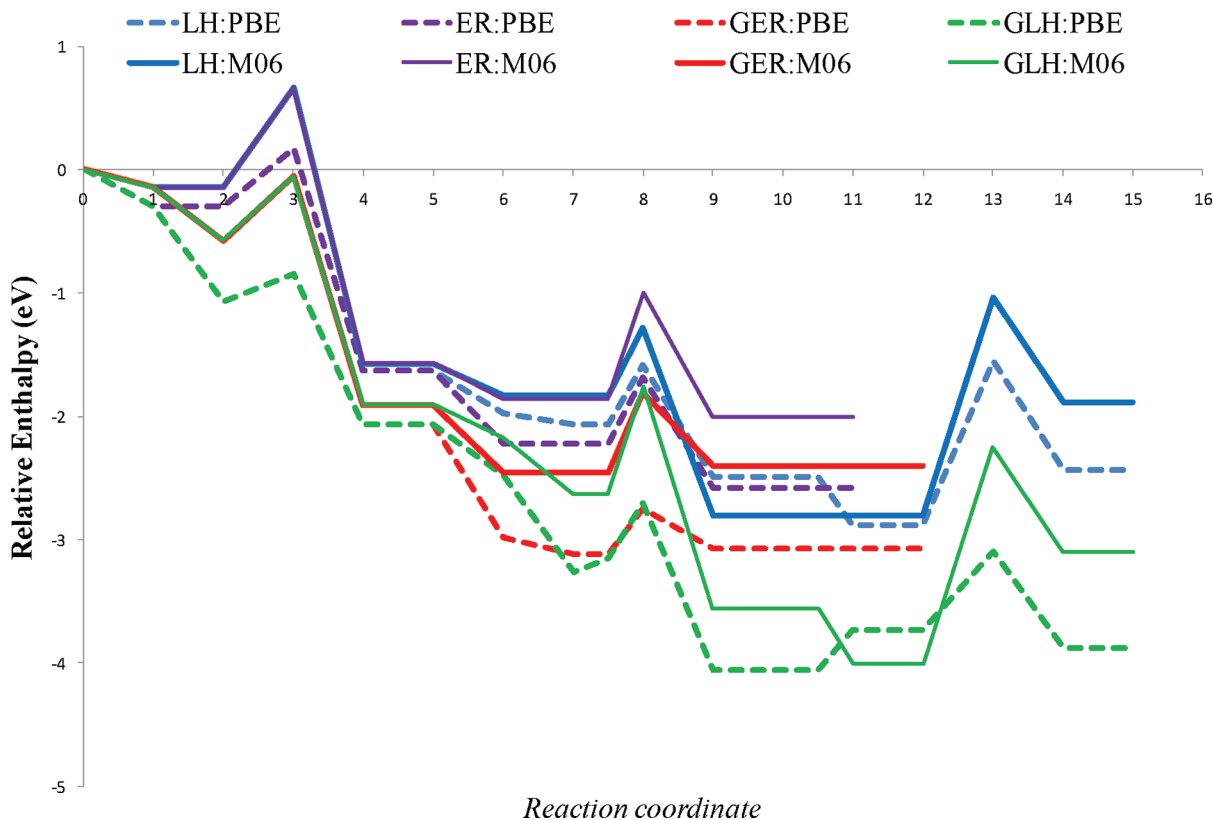


Figure 7. PBE/6-311G\*\* and M06/6-311++G\*\* reaction path energetics for  $\text{Al}_{20}^{-1}$  + water. The four mechanisms shown all result in the release of  $\text{H}_2$ .

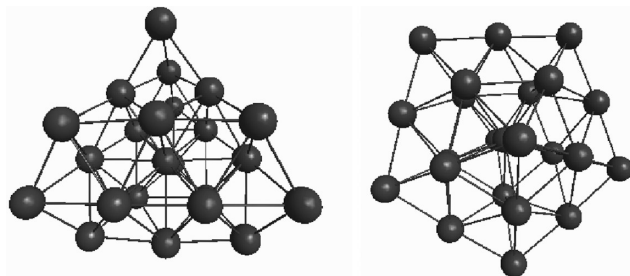


Figure 8. Structures for  $\text{Al}_{23}^{-1}$ , left to right: M2 and M3.

likely than the LH mechanism, as they avoid the third step, which has a large barrier and is endothermic.

Two reaction paths were also found for the GER mechanism, but they are mirror images of each other with no significant differences in structure or energetics. The 1.1 eV (M06: 0.6 eV) gained by the addition of the first two water molecules should be enough to get over the first bond-breaking barrier of 0.2 eV (M06: 0.5 eV). This step is exothermic by 1.0 eV (M06: 1.33 eV), and addition of the third water molecule gains another 1.1 eV (M06: 0.6 eV). The second and final step has a barrier of 0.4 eV (M06: 0.7 eV) and is approximately thermoneutral. The modest barriers and overall exothermicity of 3.1 eV (M06: 2.4 eV) make this mechanism seem quite likely.

The GLH mechanism is identical to the GER mechanism for the first step, and the barrier for its second step is similar in magnitude to the second step in the GER mechanism. However, while the second step in the GER mechanism is the  $\text{H}_2$ -producing final step, completion of the GLH mechanism to

Table 2. Relative Energies of  $\text{Al}_{23}^{-1}$  Structures

$\text{Al}_{23}^{-1}$	M2	M3
M06/6-311++G**	energy (eV)	0.39
	enthalpy (eV)	0.37
PBE/6-311G**	energy (eV)	0.00
	enthalpy (eV)	0.00
PBE/DZP	ref 14	0.00
		0.04

release  $\text{H}_2$  requires a third step, which has a significant barrier. Thus, the GER mechanism seems most likely.

The experimental data for these reactions were obtained by detecting species in the product stream by mass spectroscopy.<sup>10</sup> While the experimental report is that  $\text{Al}_{20}^{-1}$  resists reacting with water, the peak near a mass of 616 could be the GLH product,<sup>10</sup> while the GER product at a mass of 596 may be obscured by the large peak at a mass of 594 from unreacted  $\text{Al}_{22}^{-1}$ . Because the initial binding energies for these mechanisms are small, the leaving of water before reaction occurs may be competitive with the GLH and GER mechanisms outlined here, resulting in the experimentally observed slow reaction rate, even at high water concentrations.<sup>10</sup>

D.  $\text{Al}_{23}^{-1}$ . For  $\text{Al}_{23}^{-1}$ , the second and third energy-minimized structures of Aguado and Lopez,<sup>14</sup> labeled M2 and M3 in Figure 8, are close in energy, and while M2 is calculated to be the global minimum by 0.12 eV when the PBE functional is used, M3 is calculated to be the global minimum by 0.37 eV when the M06 functional is used, as shown in Table 2. Structure M2 might be called a highly distorted tetrahedron, while M3 is approximately a pentagonal bipyramid.

The reaction of each of these two structures with water has been investigated with the LH, ER, GLH, and GER mechanisms.

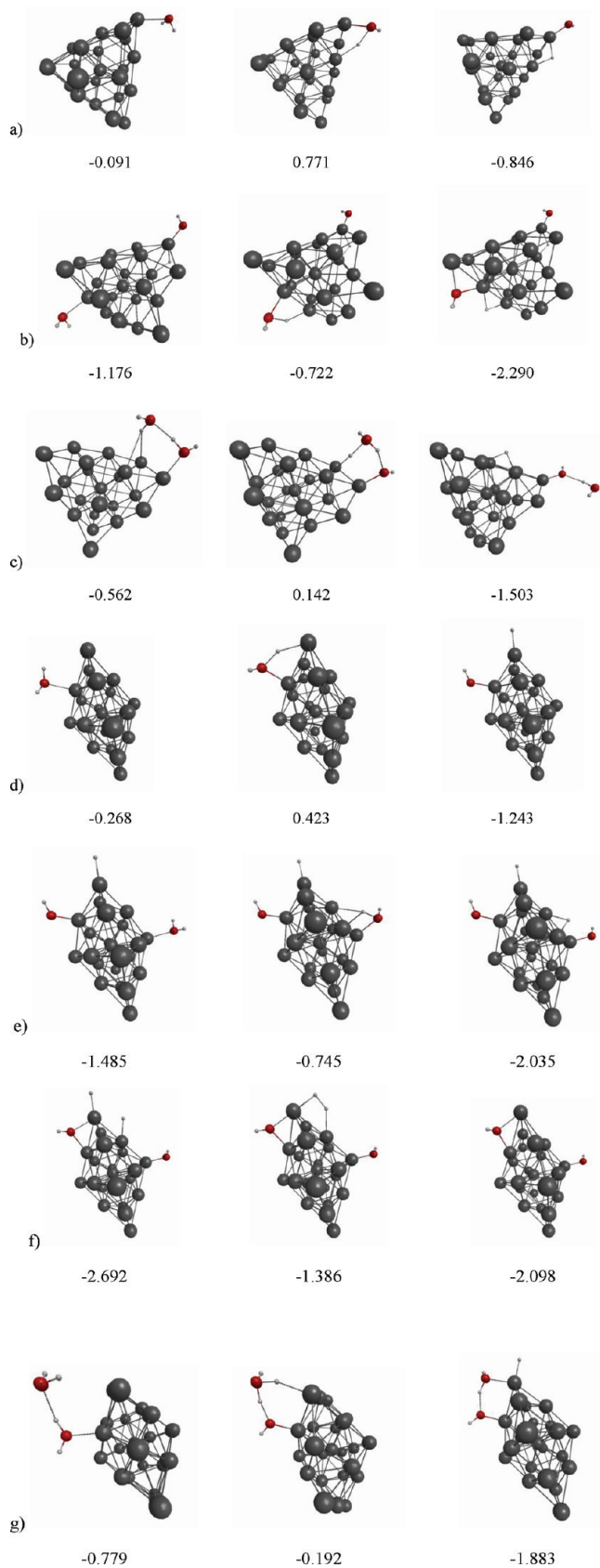
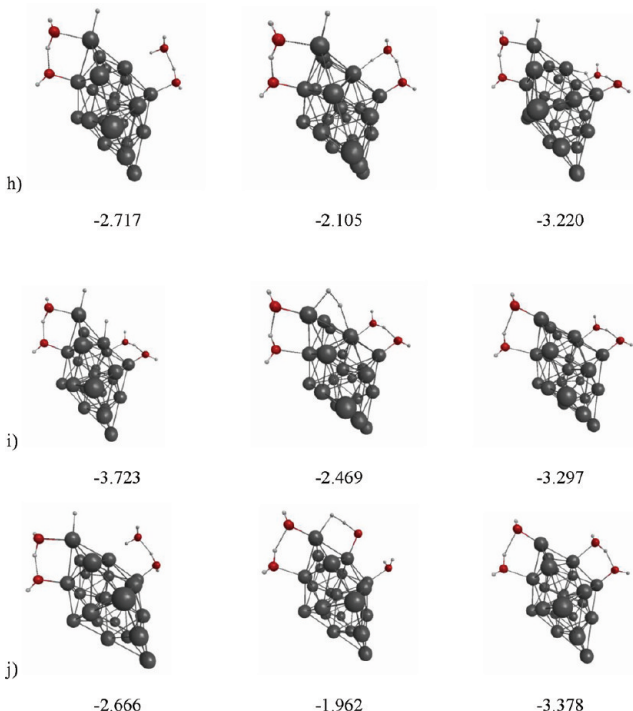


Figure 9. Continued



**Figure 9.** Reaction path structures for  $\text{Al}_{23}^{-1}$  + water. See caption for Figure 1. (a) M2 LH step 1. (b) M2 GER step 2. (c) M2 GLH step 1. (d) M3 LH step 1. (e) M3 LH step 2. (f) M3 LH step 3. (g) M3 GLH and GER step 1. (h) M3 GLH step 2. (i) M3 GLH step 3. (j) M3 GER step 2.

Figure 9 shows the structures and relative enthalpies for each step in each mechanism, and the reaction energetics are plotted in Figure 10. The first two steps of the LH mechanism for structure M2 were found, with the chemisorption of the two water molecules again driven by the presence of adjacent Lewis-acid and Lewis-base sites. The resulting two hydrogen atoms bonded to the cluster in this mechanism are too far apart to form  $\text{H}_2$ , so this mechanism fails to produce hydrogen gas. A path for the ER mechanism was not found for the M2 structure. A mechanism for the first step in a GLH or GER path was found, but a second step could not be found due to a lack of adjacent Lewis acid–Lewis base sites combined with the strong binding of the first H atom to the cluster.

When the M3 structure is used, reaction paths using the LH, GLH, and GER mechanisms were found. In the LH mechanism, the energy gained from the initial water adsorption (PBE, 0.51 eV; M06, 0.27 eV) may not be enough to surmount the barrier (PBE, 0.39 eV; M06, 0.69 eV) for the first bond splitting (particularly according to the results from the M06 functional), so this mechanism is likely to be slow except at high temperature. However, because this step is exothermic by about 1 eV, and adsorption of the second water molecule gains an additional 0.55 eV (M06: 0.24 eV), the system should have enough energy to get over the second barrier of 0.48 eV (M06: 0.74 eV). Because the second step is exothermic by 0.66 eV (M06: 0.55 eV) and is followed by a rearrangement that is exothermic by 0.35 eV (M06: 0.66 eV), the system may have enough energy to surmount the final barrier of 0.96 eV (M06: 1.31 eV). However, the two Grothus-type mechanisms seem more likely with their lower barriers and larger exothermicity. The GER mechanism seems particularly likely because it releases

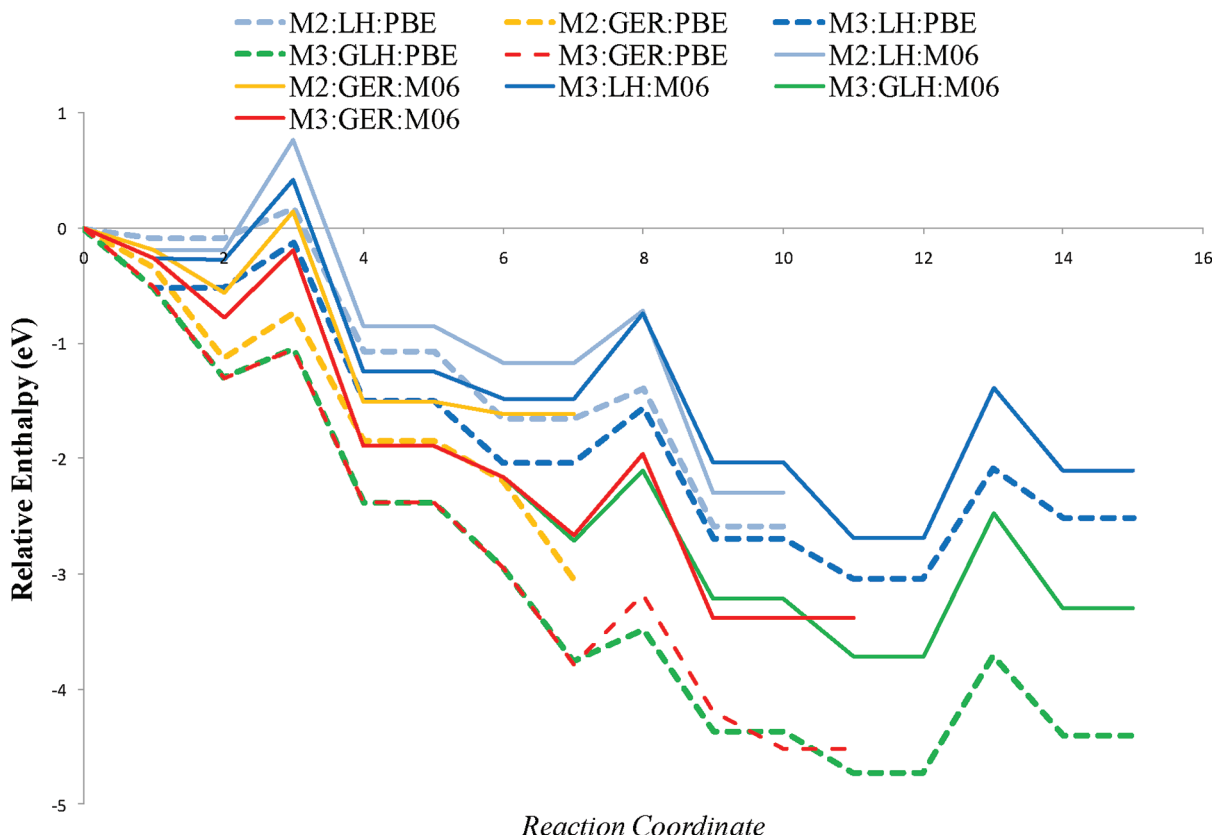


**Figure 10.** PBE/6-311G\*\* and M06/6-311++G\*\* reaction path energetics (corrected with zero-point-vibrational energies) for  $\text{Al}_{23}^{-1}$  + water. The two mechanisms starting with the M2 structure do not produce  $\text{H}_2$ , while the three mechanisms starting from the M3 structure all produce  $\text{H}_2$ .

$\text{H}_2$  after just two steps, while the third step in the GLH mechanism has a significant barrier (PBE, 1.02 eV; M06, 1.25 eV).

#### IV. CONCLUSIONS

The reaction of aluminum nanocluster anions with water has been studied theoretically using density functional theory. The results from the PBE and M06 functionals are in at least qualitative agreement, with the M06 calculations yielding somewhat larger reaction barriers. Our study did find significant size and structure specificity in reactivity. As found previously,<sup>13</sup> the superatom model is not fully reliable for predicting the properties of aluminum cluster anions. The importance of sites that act as Lewis acids and Lewis bases, as described previously,<sup>9,10</sup> was confirmed. The Grotthuss-like mechanisms, where additional water molecules facilitate the proton transfer reaction, were shown to be important paths for these reactions. For the  $\text{Al}_{12}^{-1}$  cluster, a Grotthuss-like mechanism for  $\text{H}_2$  production could not be found. However, an ER mechanism was found, as well as a second LH mechanism that could release  $\text{H}_2$ . The LH mechanism found previously<sup>9,10</sup> was confirmed with both functionals, and due to the low barrier in its second step and particularly stable product, may be the reason for the experimental result, indicating that this cluster does not lead to  $\text{H}_2$  production. For the  $\text{Al}_{17}^{-1}$  cluster, the previously found LH mechanism was extended to release a second  $\text{H}_2$  molecule, and two other  $\text{H}_2$ -producing mechanisms were found that use Grotthus-like mechanisms. The products of these mechanisms can also be observed in the experimental data.<sup>9,10</sup> For the  $\text{Al}_{20}^{-1}$  cluster, four mechanisms were found, but only the two Grotthuss-like mechanisms are likely to be

energetically feasible except at high temperature, and they may only play a major role at larger water concentrations. These factors may explain the resistance to reactivity of this cluster observed experimentally. For the  $\text{Al}_{23}^{-1}$  cluster, the initial binding energy is larger, which may explain its enhanced reactivity. The experiment did not report whether  $\text{H}_2$  was produced in the reaction of  $\text{Al}_{23}^{-1}$  with water, yet the results of this study indicate that the M3 structure is likely to produce  $\text{H}_2$ , but that the M2 structure might not produce  $\text{H}_2$  even though it reacts with water. Our analysis has provided a more complete understanding of hydrogen production by Al anion clusters than previously reported, consistent with experimental results that are available so far.

#### ASSOCIATED CONTENT

**S Supporting Information.** Small-cluster cohesive energies and dissociation energies of Table S1, along with Cartesian coordinates for the clusters, transition states, and products in the reactions given. This material is available free of charge via the Internet at <http://pubs.acs.org>.

#### AUTHOR INFORMATION

##### Corresponding Author

\*E-mail: paul.day@wpafb.af.mil (P.N.D.), ruth.pachter@wpafb.af.mil (R.P.).

##### Notes

The authors declare no competing financial interest.

**■ ACKNOWLEDGMENT**

We gratefully acknowledge support from AFOSR and from AFRL Section 219 funding, through a grant to Dr. Christopher Bunker, AFRL/RZ.

**■ REFERENCES**

- (1) Huang, Y.; Risha, G. A.; Yang, V.; Yetter, R. A. *Combust. Flame* **2009**, *156*, 5.
- (2) Shimojo, F.; Nakano, A.; Kalia, R. K.; Vashishta, P. *Appl. Phys. Lett.* **2009**, *95*, 043114.
- (3) Knight, W. D.; Clemenger, K.; deHeer, W. A.; Saunders, W. A.; Chou, M. Y.; Cohen, M. L. *Phys. Rev. Lett.* **1984**, *52*, 2141.
- (4) Ekardt, W. *Phys. Rev. Lett.* **1984**, *52*, 1925.
- (5) Ekardt, W. *Phys. Rev. B: Condens. Matter Mater. Phys.* **1984**, *29*, 1558.
- (6) de Heer, W. A. *Rev. Mod. Phys.* **1993**, *65*, 611.
- (7) Leuchtner, R. E.; Harms, A. C.; Castleman, A. W. J. *J. Chem. Phys.* **1989**, *91*, 2753.
- (8) Martins, J. L.; Car, R.; Buttet, J. *Surf. Sci.* **1981**, *106*, 265.
- (9) Roach, P. J.; Woodward, W. H.; Castleman, A. W., Jr.; Reber, A. C.; Khanna, S. N. *Science* **2009**, *323*, 492.
- (10) Reber, A. C.; Khanna, S. N.; Roach, P. J.; Woodward, W. H.; Castleman, A. W., Jr. *J. Phys. Chem. A* **2010**, *114*, 6071.
- (11) Shimojo, F.; Ohmura, S.; Kalia, R. K.; Nakano, A.; Vashishta, P. *Phys. Rev. Lett.* **2010**, *104*, 126102.
- (12) Ohmura, S.; Shimojo, F.; Kalia, R. K.; Kunaseth, M.; Nakano, A.; Vashishta, P. *J. Chem. Phys.* **2011**, *134*, 244702.
- (13) Ma, L.; Issendorff, B. v.; Aguado, A. *J. Chem. Phys.* **2010**, *132*, 104303.
- (14) Aguado, A.; López, J. M. *J. Chem. Phys.* **2009**, *130*, 064704.
- (15) Perdew, J. P.; Burke, K.; Ernzerhof, M. *Phys. Rev. Lett.* **1996**, *77*, 3865.
- (16) Ernzerhof, M.; Scuseria, G. E. *J. Chem. Phys.* **1999**, *110*, 5029.
- (17) Drebov, N.; Ahlrichs, R. *J. Chem. Phys.* **2011**, *134*, 124308.
- (18) Zhao, Y.; Truhlar, D. G. *Theor. Chem. Acc.* **2008**, *120*, 215.
- (19) Schmidt, M. W.; Baldridge, K. K.; Boatz, J. A.; Elbert, S. T.; Gordon, M. S.; Jensen, J. H.; Koseki, S.; Matsunaga, N.; Nguyen, K. A.; Su, S.; Windus, T. L.; Dupuis, M.; Montgomery, J. A. *J. Comput. Chem.* **1993**, *14*, 1347.
- (20) Frisch, M. J.; Trucks, G. W.; Schlegel, H. B.; Scuseria, G. E.; Robb, M. A.; Cheeseman, J. R.; Scalmani, G.; Barone, V.; Mennucci, B.; Petersson, G. A.; Nakatsuji, H.; Caricato, M.; Li, X.; Hratchian, H. P.; Izmaylov, A. F.; Bloino, J.; Zheng, G.; Sonnenberg, J. L.; Hada, M.; Ehara, M.; Toyota, K.; Fukuda, R.; Hasegawa, J.; Ishida, M.; Nakajima, T.; Honda, Y.; Kitao, O.; Nakai, H.; Vreven, T.; Montgomery, J. A., Jr.; Peralta, J. E.; Ogliaro, F.; Bearpark, M.; Heyd, J. J.; Brothers, E.; Kudin, K. N.; Staroverov, V. N.; Keith, T.; Kobayashi, R.; Normand, J.; Raghavachari, K.; Rendell, A.; Burant, J. C.; Iyengar, S. S.; Tomasi, J.; Cossi, M.; Rega, N.; Millam, J. M.; Klene, M.; Knox, J. E.; Cross, J. B.; Bakken, V.; Adamo, C.; Jaramillo, J.; Gomperts, R.; Stratmann, R. E.; Yazyev, O.; Austin, A. J.; Cammi, R.; Pomelli, C.; Ochterski, J. W.; Martin, R. L.; Morokuma, K.; Zakrzewski, V. G.; Voth, G. A.; Salvador, P.; Dannenberg, J. J.; Dapprich, S.; Daniels, A. D.; Farkas, O.; Foresman, J. B.; Ortiz, J. V.; Cioslowski, J.; Fox, D. J. *Gaussian 09*, revision B.01; Gaussian, Inc.: Wallingford, CT, 2010.
- (21) Baker, J. J. *Comput. Chem.* **1986**, *7*, 385.
- (22) Helgaker, T. *Chem. Phys. Lett.* **1991**, *182*, 503.
- (23) Culot, P.; Dive, G.; Nguyen, V. H.; Ghysen, J. M. *Theor. Chim. Acta* **1992**, *82*, 189.
- (24) Gonzalez, C.; Schlegel, H. B. *J. Chem. Phys.* **1989**, *90*, 2154.
- (25) Kozuch, S.; Shaik, S. *J. Am. Chem. Soc.* **2006**, *128*, 3355.